Inorg. Chem. **2008**, *47*, 9327−9332

Strong Rail Spin $^1/_2$ Antiferromagnetic Ladder Systems: (Dimethylammonium)(3,5-Dimethylpyridinium)CuX_4, X = Cl, Br

Firas Awwadi,[†] Roger D. Willett,*[,‡] Brendan Twamley,[§] Ryan Schneider,[||] and Christopher P. Landee[||]

Department of Chemistry, Tafila Technical University, Tafila, 66110 Jordan, Department of Chemistry, Washington State University, Pullman, Washington 99164, University Research Office, University of Idaho, Moscow, Idaho 83844, and Department of Physics, Clark University, Worcester, Massachusetts 01610

Received May 18, 2008

The mixed cation salts, (dimethylammonium)(3,5-dimethylpyridinium)CuX_4 (X = Cl, Br), henceforth (DMA)-(35DMP)CuX_4, are new examples of spin-ladders based on nonbonded halide···halide interactions between CuX_4^{2-} anions. In these structures, double rows of the CuX_4^{2-} anions are sheathed by the $35DMP^+$ cations, while the edges are capped by the DMA^+ cations. For the Br salt, the Br···Br contacts that define the rungs of the ladder are 4.017 Å in length, while those that define the rails are 3.983 Å. For the Cl salt, the corresponding lengths are 3.967 and 4.045 Å. The susceptibility data for the Br salt exhibits a maximum at ∼5.5 K, and fitting the data to the spin $^1/_2$ antiferromagnetic ladder model yields $2J(\text{rail})/k = -7.95$ K and $2J(\text{rung})/k = -4.07$ K. The exchange coupling is much weaker in the Cl salt, no maximum in χ is observed down to 1.8 K, and the corresponding exchange constants are −1.59 and −1.25 K, respectively. An analysis is made of the structural factors involved in the *J*(rung) pathway.

Introduction

A large number of significant and novel spin-$^1/_2$ Heisenberg magnetic systems based on copper(II) halide salts continue to be synthesized and studied. These include a series of structures with two-dimensional ferromagnetic interactions based on the $(RNH_3)_2CuX_4$ layer perovskite structures,[1] the first examples of systems with one-dimensional ferromagnetic interactions,[2] as well as systems which exhibit one- and two- dimensional antiferromagnetic behavior.[2c,3] Because of the structural flexibility of the copper(II) halide coordination sphere and of the Cu−X−Cu linkages, a seemingly endless plethora of spin-$^1/_2$ Heisenberg systems has been investigated. There is a renewed interest in the study of the magnetic behavior of copper(II) halide compounds because of the interest in complex magnetic systems, such as spin ladders,[4] alternating exchange chains,[5] and frustrated systems.[6]

* To whom correspondence should be addressed. E-mail: rdw@mail.wsu.edu.
[†] Tafila Technical University.
[‡] Washington State University.
[§] University of Idaho.
[||] Clark University.

(1) (a) De Jongh, L. J.; Miedema, A. R. *Adv. Phys.* **1974**, *23*, 1. (b) Steadman, J. P.; Willett, R. D. *Inorg. Chim. Acta* **1970**, *4*, 367. (c) Barendregt, F.; Schenk, H. *Physica* **1970**, *49*, 465. (d) Willett, R. D. *Acta Crystallogr.* **1990**, *C46*, 565. (e) Tichy, K.; Benes, J.; Holg, W.; Arend, H. *Acta Crystallogr.* **1978**, *B34*, 2970. (f) Middleton, M.; Place, H.; Willett, R. D. *J. Am. Chem. Soc.* **1988**, *110*, 8639. (g) Landee, C. P.; Halvorson, K.; Willett, R. D. *J. Appl. Phys.* **1987**, *61*, 3295.

(2) (a) Willett, R. D.; Landee, C.; Swank, D. D. *J. Appl. Phys.* **1978**, *49*, 1329. (b) Swank, D. D.; Landee, C. P.; Willett, R. D. *Phys. Rev. B.* **1979**, *20*, 2154. (c) Landee, C. P.; Willett, R. D. *Phys. Rev. Lett.* **1979**, *43*, 463. (d) Willett, R. D.; Landee, C. P.; Gaura, R. M.; Swank, D. D.; Groenendijk, H.; van Duyneveldt, A. J. *J. Magn. Magn. Mater.* **1980**, *15*−*18*, 1055. (e) Landee, C. P.; Willett, R. D. *J. Appl. Phys.* **l981**, *52*, 2240. (f) Landee, C. P.; Willett, R. D. *J. Phys. (Paris)* **1978**, *39*, 741.

(3) (a) Woodward, F. M.; Albrecht, A. S.; Wynn, C. M.; Landee, C. P.; Turnbull, M. M. *Phys. Rev. B* **2002**, *65*, 144121-1-13. (b) Woodward, F. M.; Landee, C. P.; Giantsidis, J.; Turnbull, M. M.; Richardson, C. *Inorg. Chim. Acta* **2001**, *324*, 324.

(4) (a) Patyal, B. R.; Scott, B.; Willett, R. D. *Phys. Rev. B* **1990**, *41*, 1657. (b) Watson, B. C.; Kotov, V. N.; Meisel, M. W.; Hall, D. W.; Granoth, G. E.; Montfrooij, W. T.; Nagler, S. E.; Jensen, D. A.; Backov, R.; Petruska, M. A.; Fanucci, G. E.; Talham, D. R. *Phys. Rev. Lett.* **2001**, *86*, 5168. (c) Landee, C. P.; Turnbull, M. M.; Galeriu, C.; Giantsidis, J.; Woodward, F. M. *Phys. Rev. B, Rapid Commun.* **2001**, *63*, 100402R. (d) Turnbull, M. M.; Galeriu, C.; Giantsidis, J.; Landee, C. P. *Mol. Cryst. Liq. Cryst.* **2002**, *376*, 469. (e) Willett, R. D.; Galeriu, C.; Landee, C. P.; Turnbull, M. M.; Twamley, B. *Inorg. Chem.* **2004**, *43*, 3804. (f) Shapiro, A.; Landee, C. P.; Turnbull, M. M.; Jornet, J.; Deumal, M.; Novoa, J. J.; Robb, M.; Lewis, W. *J. Am. Chem. Soc.* **2007**, *129*, 952.

(5) (a) Vasilevesky, I.; Rose, N. R.; Steinkamp, R.; Willett, R. D. *Inorg. Chem.* **1991**, *30*, 4082. (b) Willett, R. D.; Wang, Z.; Molnar, S.; Brewer, K.; Landee, C. P.; Turnbull, M. M.; Zhang, W. *Mol. Cryst. Liq. Cryst.* **1993**, *233*, 277.

10.1021/ic800905e CCC: $40.75
Published on Web 09/25/2008

The study of the magneto-structural correlations in the single halide Cu−X−Cu pathways that occur in these systems has been a major area of activity in the past several decades.[7] In addition to systems that contain single-halide exchange pathways, it has been shown that significant antiferromagnetic exchange coupling can occur through so-called two-halide exchange pathways that involve contacts between halide ions on neighboring copper(II) centers. This was clearly demonstrated for the diammonium $(NH_3RNH_3)CuX_4$ layer perovskite series where the antiferromagnetic coupling between the eclipsed ferromagnetic perovskite layers increases exponentially as the length of the diammonium cation (and thus the interlayer X···X distance) decreases.[8] A class of compounds where significant antiferromagnetic coupling can exist is the A_2CuX_4 salts that contain tetrahedral CuX_4^{2-} anions. Depending on the steric and hydrogen bonding capabilities of the A^+ cations, a variety of magnetic systems have been made that had previously been inaccessible experimentally.[9] Significantly, it has been shown that the experimental exchange coupling in these systems can be reproduced quite accurately theoretically.[10] Another class of compounds where these interactions are proving to be important are the $Cu_2X_6^{2-}$ dimer systems.[11]

The reason for the existence of significant 2X coupling in copper(II) halide systems can be easily understood from the analysis of EPR data on these systems, which shows that the unpaired electron density is significantly delocalized from the Cu d-orbitals into the σ ligand orbitals.[12] This delocalization is exceptionally large because of the near match in energies for the Cu d-orbitals and the ligand highest occupied molecular orbitals (HOMOs). Because this energy difference is less for X = Br than for X = Cl, the delocalization is greater for the bromide salts, and thus, the role of the two-halide exchange is expected (and observed) to be greater for the bromide systems.

A class of systems of current interest where copper halide salts play a significant role is that of magnetic ladders with varying ratios of J_{rung}/J_{rail}.[4,13] The magnetic model of a spin ladder is relatively recent.[14] Such ladders consist of two parallel chains with intrachain exchange strengths, J_{rail}, which are linked to each other by a second interaction, J_{rung}. The most interesting case occurs when both interactions are antiferromagnetic. Interest in the physics community grew after it was realized that the ground state was a spin singlet induced by and proportional to J_{rung}, no matter how large the ratio J_{rail}/J_{rung}. In our continuing study of the structural and magnetic behavior of copper(II) halide systems, we report in this paper the properties of the compounds (DMA)(35DBP)CuX_4 (where DMA^+ is the dimethylammonium cation, $35DMP^+$ is the 3,5-dimethylpridinium cation). The crystal structure analysis reveals that the X···X contacts define a spin-ladder system, and the analysis of the magnetic data shows that it behaves as a strong-rail antiferromagnetic ladder.

Experimental Section

Crystals of the (DMA)(35DMP)CuX_4 compounds were grown by evaporation of an aqueous solution containing a 1:1:1 ratio of (DMA)X, (35DMP)X, and the corresponding copper(II) halide salt. A few drops of the hydrohalic acid were added to the solution to avoid hydrolysis of the Cu(II) ion.

X-ray Diffraction. Crystals of the compounds were removed from the flask and covered with a layer of hydrocarbon oil. A suitable crystal of each compound was selected, attached to a glass fiber, and placed in the low-temperature nitrogen stream. Data were collected on both compounds at 83(2) K using a Bruker/Siemens SMART APEX instrument (Mo Kα radiation, $\lambda = 0.71073$ Å) equipped with a Cryocool NeverIce low temperature device. Data were measured using omega scans of 0.3° per frame for 5 s, and a hemisphere of data was collected. A total of 1471 frames were collected with a final resolution of 0.77 Å. The first 50 frames were recollected at the end of data collection to monitor for decay. Cell parameters were retrieved using the SMART software[15] and refined using SAINTPlus on all observed reflections.[16] Data reduction and correction for Lp and decay were performed using the SAINTPlus software. Absorption corrections were applied using SADABS.[17] The structure was solved by direct methods and refined by least-

(6) (a) Stone, M. B.; Zaliznyak, I.; Reich, D. H.; Broholm, C. *Phys. Rev. B* **2001**, *64*, 144405. (b) Stone, M. B.; Zaliznyak, I. A.; Hong, T.; Broholm, C. L.; Reich, D. H. *Nature* **2006**, *440*, 187. (c) Cavadini, N.; Rüegg, Ch.; Furrer, A.; Güdel, H.-U.; Krämer, K.; Mutka, H.; Vorderwisch, P. *Phys. Rev. B* **2002**, *65*, 132415. (d) Cavadini, N.; Heigold, G.; Henggeler, W.; Furrer, A.; Güdel, H.-U.; Krämer, K.; Mutka, H. *J. Phys., Condens. Matter* **2000**, *12*, 5463.

(7) (a) Willett, R. D. *Inorg. Chem.* **1986**, *25*, 1918. (b) O'Brien, S.; Gaura, R. M.; Landee, C. P.; Ramakrishna, B. L.; Willett, R. D. *Inorg. Chim. Acta* **1987**, *141*, 83. (c) Grigereit, T.; Drumheller, J. E.; Scott, B.; Pon, G.; Willett, R. D. *J. Magn. Magn. Mater.* **1992**, *104−107*, 1981.

(8) (a) Halvorson, K.; Willett, R. D. *Acta Crystallogr.* **1988**, *C44*, 2071. (b) Block, R.; Jansen, L. *Phys. Rev. B* **1982**, *26*, 148. (c) Rubenacker, G. V.; Waplak, S.; Hutton, S. L.; Haines, D. N.; Drumheller, J. E. *J. Appl. Phys.* **1985**, *57*, 3341. (d) Snively, L. O.; Haines, D. N.; Emerson, K.; Drumheller, J. E. *Phys. Rev. B* **1982**, *26*, 5245. (e) Snively, L. O.; Seifert, P. L.; Emerson, K.; Drumheller, J. E. *Phys. Rev. B* **1979**, *20*, 2101. (f) Snively, L. O.; Tuthill, G.; Drumheller, J. E. *Phys. Rev. B* **1981**, *24*, 5349.

(9) (a) Turnbull, M. M.; Landee, C. P.; Wells, B. M. *Coord. Chem. Rev.* **2005**, *249*, 2567. (b) Zhou, P.; Drumheller, J. E.; Rubenacker, G. V.; Halvorson, K.; Willett, R. D. *J. Appl. Phys.* **1991**, *69*, 5804. (c) Lee, Y.-M.; Park, S.-M.; Kang, S. K.; Kim, Y.-I.; Choi, S.-N. *Bull. Korean Chem. Soc.* **2004**, *25*, 823.

(10) Deumal, M.; Giorgi, G.; Robb, M. A.; Turnbull, M. M.; Landee, C. P.; Novoa, J. J. *Eur. J. Inorg. Chem.* **2005**, 4697.

(11) (a) Willett, R. D.; Twamley, B.; Montfrooij, W.; Granroth, G. G.; Nagler, S. E.; Hall, D. W.; Park, J.-H.; Watson, B. C.; Meisel, M. W.; Talham, D. R. *Inorg. Chem.* **2006**, *45*, 7689. (b) Willett, R. D.; Butcher, R.; Landee, C. P.; Twamley, B. *Polyhedron* **2005**, *24*, 2222. (c) Butcher, R.; Willett, R. D.; Landee, C. P.; Twamley, B. *Polyhedron* **2006**, *25*, 2093.

(12) Chow, C.; Willett, R. D. *J. Chem. Phys.* **1973**, *59*, 2620.

(13) (a) Luque, A.; Sertucha, J.; Lezama, L.; Rojo, T.; Roman, P. *J. Chem. Soc., Dalton Trans.* **1997**, 847. (b) Watson, B. C.; Kotov, V. N.; Meisel, M. W.; Hall, D. W.; Granoth, G. E.; Montfrooij, W. T.; Nagnler, S. E.; Jensen, D. A.; Backov, R.; Petruska, M. A.; Fanucci, G. E.; Talham, D. R. *Phys. Rev. Lett.* **2001**, *86*, 5168. (c) Landee, C. P.; Turnbull, M. M.; Galeriu, C.; Giantsidis, J.; Woodward, F. M. *Phys. Rev. B, Rapid Commun.* **2001**, *63*, 100402R. (d) Turnbull, M. M.; Galeriu, C.; Giantsidis, J.; Landee, C. P. *Mol. Cryst. Liq. Cryst.* **2002**, *376*, 469.

(14) (a) Dagotto, E.; Rice, T. M. *Science* **1996**, *271*, 618. (b) Dagotto, E. *Rep. Prog. Phys.* **1999**, *62*, 1525. (c) Barnes, T.; Dagotto, E.; Riera, J.; Swanson, E. S. *Phys. Rev. B* **1993**, *47*, 3196. (d) Dagotto, E.; Riera, J.; Scalapino, D. J. *Phys. Rev. B* **1992**, *45*, 5744. (e) Nagato, T.; Uehara, M.; Goto, J.; Akimitsu, J.; Motoyama, N.; Eisaki, H.; Uchida, S.; Takahashi, H.; Nakanishi, T.; Mori, N. *Phys. Rev. Lett.* **1998**, *81*, 1090. (f) Dhalenne, A.; Revcolevschi, R. *Science* **1998**, *279*, 345.

(15) *SMART*, v. 5.632; Bruker AXS: Madison, WI, 2005.

(16) *SAINTPlus, Data Reduction and Correction Program*, v. 7.23a; Bruker AXS: Madison, WI, 2004.

Table 1. Crystallographic Data Collection and Refinement Parameters

compound	(DMA)(35DMP) $CuBr_4$	(DMA)(35DMP) $CuCl_4$
empirical formula	$C_9H_{18}Br_4CuN_2$	$C_9H_{18}Cl_4CuN_2$
formula weight	537.43	359.59
temperature	85(2) K	83(2) K
wavelength	0.71073 Å	0.71073 Å
crystal system	triclinic	triclinic
space group	$P\bar{1}$	$P\bar{1}$
a (Å)	7.4593(15)	7.2437(4)
b (Å)	8.2697(17)	8.0952(4)
c (Å)	13.720(3)	13.3993(7)
α (deg)	107.41(3)	72.583(1)
β (deg)	90.21(3)	89.708(1)
γ (deg)	91.37(3)	88.240(1)
V(Å^3)	807.3(3)	749.34(7)
Z	2	2
ρ_{calc} (Mg/m^3)	2.211	1.594
μ (mm^{-1})	11.232	2.147
reflections collected	7248	9675
independent reflections	3697 [R(int) = 0.0239]	4123 [R(int) = 0.0222]
goodness-of-fit on F^2	1.006	1.041
R_1, wR_2 [$I > 2\sigma(I)$][a,b]	0.0300, 0.0743	0.0260, 0.0662
R_1, wR_2 (all data)[a,b]	0.0361, 0.0770	0.0291, 0.0677
largest diff. peak and hole (e Å^{-3})	1.113 and −0.742	0.508 and −0.42

[a] $R_1 = \sum||F_o| - |F_c||/\sum|F_o|^2$. [b] $wR_2 = \{\sum[w(F_o^2 - F_c^2)^2/\sum[w(F_c^2)^2]\}^{1/2}$.

squares method on F^2 using the SHELXTL program package.[18] All non-hydrogen atoms were refined anisotropically. No decomposition was observed during data collection. Details of the data collection and refinement are given in Table 1, and the asymmetric unit isillustrated in Figure 1. Further details are provided in the Supporting Information.

Magnetic Studies. The susceptibility studies were done on crushed single crystal samples using a Quantum Design MPMS SQUID Magnetometer. The magnetization of the sample was first determined as a function of field at 1.8 K and found to be linear up to 2 T. No hysteresis was detected. For the determination of the molar magnetic susceptibility χ_{mol}, the magnetic moments of the compounds were determined in fields of 1 T (Br) or 1 kOe (Cl) as a function of temperature between 2.0 and 300 K. Corrections to the molar susceptibility have been made for the temperature independent magnetization of the Cu(II) ion, and the diamagnetic contribution was calculated from Pascal's constants.

Structural Description

These novel mixed-cation structures consist of discrete DMA^+ and $35DMP^+$ cations and CuX_4^{2-} anions, as seen in Figure 1 for the bromide salt. The isolated CuX_4^{2-} anions show a typical D_{2d} compressed distortion of the tetrahedra. For the Br salt, Cu−Br = 2.386 Å (ave.) and *trans* Br−Cu−Br = 136.9° (ave.). The corresponding values for the Cl salt are 2.255 Å and 137.8°, respectively. The $35DMP^+$ cations form stacks along the a axis, as shown in Figure 2 for the bromide salt, in which adjacent cations are related by centers of inversion. The pyridinium rings of the lower pair in Figure 2a (labeled **A** and **B**) are nearly eclipsed, with $d_\perp$ = 3.419 Å and d_C = 3.699 Å ($d_\perp$ is the distance between the planes of the pyridinium rings and d_C is the

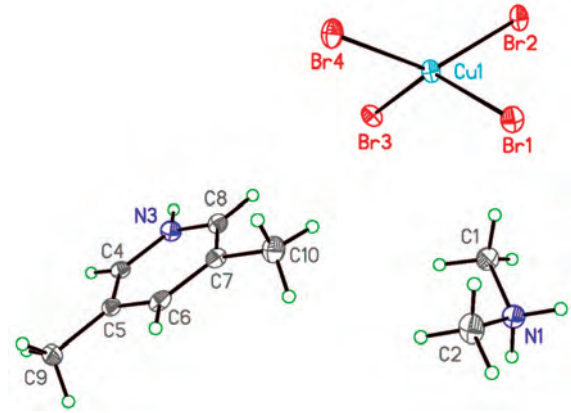

Figure 1. Asymmetric unit and atom labeling for (DMA)(35DMP)$CuBr_4$.

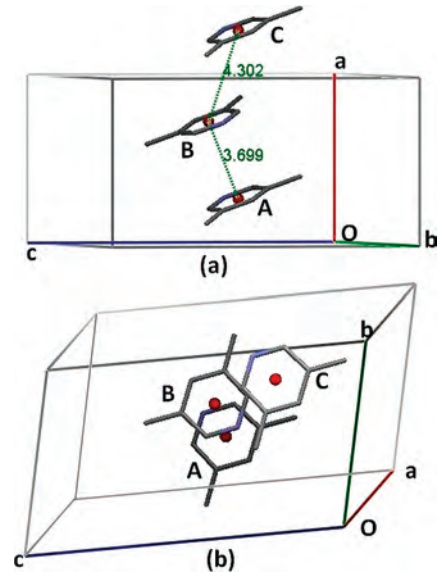

Figure 2. (a) Illustration of the π-π stacking of the $35DMP^+$ cations in the bromide salt. The stacks are parallel to the a axis. The red balls are located at the centroids of the pyridinium rings. (b) View normal to the plane of the pyridinium rings.

distance between centroids). The centroids of the pyridinium rings in the upper pair in Figure 2a (labeled **B** and **C**) are displaced more, with $d_\perp$ = 3.400 Å and d_C = 4.302 Å. The corresponding values in the chloride salt are $d_\perp$ = 3.365 Å and d_C = 3.599 Å and $d_\perp$ = 3.357 Å and d_C = 4.139 Å, respectively.

The combination of N−H···X$^-$ interactions and π-π stacking of cations **A** and **B** leads to a ladder arrangement of the CuX_4^{2-} anions based on X···X contacts (shown in Figure 3a for the bromide salt). Details of the contact parameters are given in Table 2. The contact distances along the rungs and the rails are essentially equal in each salt. In spite of this, the angular parameters defining the contacts are significantly different. The centrosymmetric geometry of the rung contacts dictate that those two Cu−X···X angles are equal (∼156° for both salts) and that the Cu−X···X-Cu dihedral angle be 180°. In contrast, for the contacts along the rail, one Cu−X···X angle is nearly linear and the other much smaller (∼137° for both salts), and the dihedral angle is now close to 90°. It is interesting that, despite the difference in ionic radii of the chloride and bromide ions,

(17) *SADABS, Empirical Absorption Correction Program*, v.2007/4; Bruker AXS: Madison, WI, 2007.
(18) Sheldrick, G.M. *SHELXTL, Structure Determination Software Suite*, v. 6.14; Bruker AXS: Madison, WI, 2004.

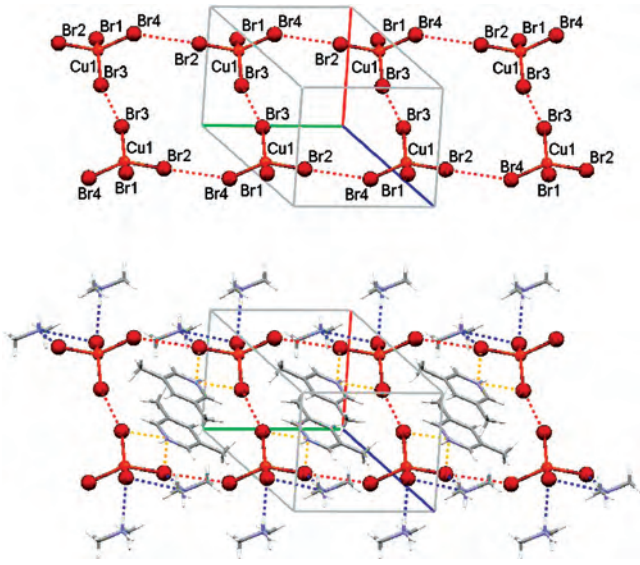

Figure 3. Illustrations of the ladder chain (a, upper) and the hydrogen bonding (b, lower) in the Br salt. Br···Br contacts are depicted by red dotted lines, hydrogen bonds from the DMA^+ cations by blue dotted lines, and hydrogen bonds from the $35DMP^+$ cations by orange dotted lines.

the X···X contact distances are essentially identical in the two salts. This suggests that the packing of the anions is largely dictated by the packing of the organic cations.

The ladders are stabilized by hydrogen bonds from the two types of organic cations, as shown in Figure 3b. Pairs of π-π stacked $35DMP^+$ cations form bifurcated hydrogen bonds to two CuX_4^{2-} anions across the diagonal of the ladder. Each DMA^+ cation forms a linear N−H···X hydrogen bond to one ladder and an asymmetric hydrogen bond to an adjacent ladder. In this way, each rung of the ladder is capped by pairs of DMA^+ cations, effectively isolating adjacent ladders (see Figure 3b).

The structural reports of mixed-cation salts in hybrid organic−inorganic materials are relatively rare. Perhaps the most common type of mixed cation systems involving organic cations are ones that contain one metal (or ammonium) ion and one organic cation, such as in $Na[N(CH_3)_4]_7[Si_8O_{20}]\cdot 54H_2O$,[19] $[(CH_3)_4N][Na][Fe(CN)_5(NO)]\cdot 2.5H_2O$,[20] and $[Li(H_2O)_4]_2[N(CH_3)_4]_4[V_{10}O_{28}]\cdot 4H_2O$.[21] These are more apt to be found than compounds where two different types of organic cations are involved. Some of these systems are found when redox processes involving the cations occur during the preparation process as in the case of $[NH_2C(I)=NH_2]_2NH_2C(H)=NH_2SnI_5$[22] and (5-Bromo-3-methyl-2-aminopyridinium)(3-methyl-2-aminopyridinium)$CuBr_4$.[23] Few systematic attempts to prepare mixed cation systems appear to have been made. One notable exception is the series of $[CH_3(CH_2)_nNH_3]_2(CH_3NH_3)_{n-1}Sn_nI_{3n+1}$ conducting layer perovskite salts prepared by Mitzi and co-workers.[24]

(19) Wiebcke, M.; Koller, H. *Acta Crystallogr.* **1992**, *B48*, 449.
(20) Longridge, J. J.; Rawson, J. M.; Davies, J. E. *Acta Crystallogr.* **1997**, *C53*, 15.
(21) Zavalij, P. Y.; Chirayil, T.; Whittingham, M. S.; Pecharsky, V. K.; Jacobson, R. A. *Acta Crystallogr.* **1997**, *C53*, 170.
(22) Mitzi, D. B.; Liang, K.; Wang, S. *Inorg. Chem.* **1998**, *37*, 321.
(23) Place, H.; Willett, R. D. *Acta Crystallogr.* **1987**, *C43*, 1050.
(24) Mitzi, D. B.; Feild, C. A.; Harrison, W. T. A.; Guloy, A. M. *Nature* **1994**, *369*, 467.

Magnetic Analysis

The magnetic susceptibilities of the $(DMA)(35DMP)CuX_4$ compounds between 2 and 320 K as shown in Figures 4 and 5, with the data below 50 K shown within the inset. The behavior of the bromide salt is dominated by a rounded maximum near 5.5 K and a rapid decrease at lower temperatures. Such behavior is characteristic of low-dimensional $S = {}^1/_2$ systems with antiferromagnetic Heisenberg exchange interactions. The higher temperature data ($T > 20$ K) are well represented by the Curie−Weiss equation with a small negative intercept on the temperature axis (Curie−Weiss parameters $C = 0.405$ emu-K/mol and $\theta = -5.1$ K for the bromide salt and $C = 0.440$ emu-K/mol and $\theta = -1.3$ K for the chloride salt). The corresponding data for the chloride salt are shown in Figure 5. In this case, the exchange coupling is weaker and no maximum is observed in the χ data down to 1.8 K.

The data were fit to the theoretical prediction for a spin ladder, with three parameters (J_{rail}, J_{rung}, and C) allowed to vary independently.[25] The best fit parameters for the Br salt, $2J_{rail}/k_B = -7.95$ K, $2J_{rung}/k_B = -4.07$ K, and $C = 0.408$ emu-K/mol, give an excellent agreement with the data at all temperatures (solid line in Figure 4). The corresponding values for the Cl data are $2J_{rail}/k_B = -1.59$ K, $2J_{rung}/k_B = -1.25$ K, and $C = 0.444$ emu-K/mol (solid line in Figure 5). The factor of ~5 for the ratio of the Br/Cl exchange constants is similar to that found in other halide salts where the X···X contact distances are the same for the chloride and bromide salts.[11b,c]

For the spin ladder system, an energy gap is expected, leading to an exponential decrease in the susceptibility at very low temperature. With the observed J_{rail}/J_{rung} ratio of 1.95 for the bromide salt, the energy gap should then be less than ${}^1/_2$ of $2J_{rung}$ or less than 2 K. Thus it would be necessary to measure below 1 K to see the exponential decay of the susceptibility, which is below the limit of our instrumentation. The fit to the bromide analog data (Figure 4) does follow the data down to the lowest measured temperature, so the data is entirely consistent with the spin ladder model. Measurements at even lower temperature would be necessary for the chloride salt. Clearly the magnetic data for this compound does not establish the spin ladder nature for other models (linear chain, antiferromagnetic layers) can also describe this data, although with statistically poorer fits. Our justification for calling the chloride salt a spin ladder is its structural similarity to the bromide analog.

Magnetostructural Correlations

$(DMA)(35DMP)CuBr_4$ is the third copper bromide-based ladder system in which $|J_{rail}| \sim 2|J_{rung}|$, the other two being the $(CPA)_2CuBr_4$ salt[4e] and the $(23DMP)_2CuBr_4$ salt.[4f] As

(25) Johnston, D. C.; Troyer, M.; Miyahara, S.; Lidsky, K.; Ueda, K.; Azuma, M.; Hiroi, Z.; Takano, M.; Isobe, M.; Ueda, Y.; Korotin, M. A.; Anisimov, V. I.; Mahajan, A. V.; Miller, L. L. Magnetic Susceptibilities of Spin-${}^1/_2$ Antiferromagnetic Heisenberg Ladders and Applications to Ladder Oxide Compounds. 2000, arXiv:cond-mat/0001147v1. arXiv.org e-Print archive. http://arXiv.org/abs/cond-mat/0001147.

Table 2. Structural Parameters for X···X Contacts

		$\theta_{Cu-X\cdots X}$ (deg)	$d_{X\cdots X}$ (Å)	$\theta_{X\cdots X-Cu}$ (deg)	$\tau_{Cu-X\cdots X-Cu}$ (deg)	$\tau_{X-Cu-X\cdots X}$ (deg)	$\tau_{X\cdots X-Cu-X}$ (deg)	$2J/k$ (K)
(DMA)(35DMP)$CuBr_4$								
Cu1−Br3···Br3′−Cu1′	rung	156.3	4.017	156.3	180	142.72	−142.72	−4.07
Cu1−Br2···Br4″−Cu1″	rail	177.6	3.983	137.6	86.1	96.51	176.47	−7.95
(DMA)(35DMP)$CuCl_4$								
Cu1−Cl3···Cl3′−Cu1′	rung	155.5	3.967	155.5	180	142.71	−142.71	−1.25
Cu1−Cl2···Cl4″−Cu1″	rail	177.8	4.045	137.2	78.1	70.37	176.93	−1.95
$(23DMP)_2CuBr_4$[a]								
	rung	155.5	4.378	155.5	180	52.78	−52.78	−8.68
	rail	151.1	3.905	127.6	−2.0	178.42	−66.60	−16.85
$(CPA)_2CuBr_4$[b]								
	rung[c]	105.3	4.396	133.8	−62.5	177.26	−67.28	−5.5
		132.1	4.519	103.2	63.4	67.22	151.24	
	rail[d]	150.1	3.893	149.8	−55.9	148.66	149.35	−11.6
		151.0	3.881	148.8	64.3	145.40	142.59	

[a] Reference 4f. [b] Reference 4e. [c] Two contacts exist in each rung. [d] The contacts in the two rails are slightly different.

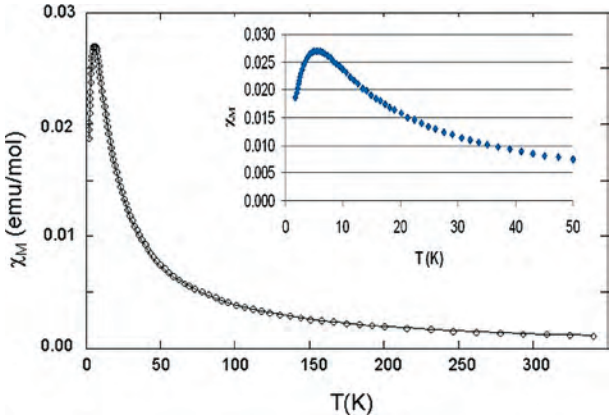

Figure 4. Magnetic susceptibility of (DMA)(35DMP)$CuBr_4$. The solid line corresponds to the spin ladder fit with the parameters $J_{rail}/k = -7.95$ K and $J_{rung}/k = -4.07$ K. The inset shows the data in the low temperature regime.

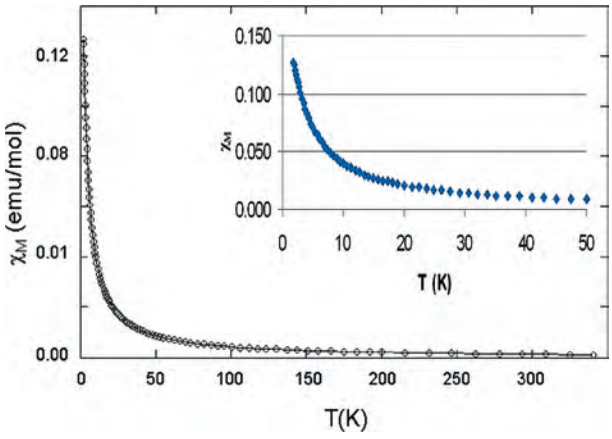

Figure 5. Magnetic susceptibility of (DMA)(35DMP)$CuCl_4$. The solid line corresponds to the spin ladder fit with the parameters $J_{rail}/k = -1.59$ K and $J_{rung}/k = -1.25$ K. The inset shows the data in the low temperature regime.

seen in Table 2, the J values for the $23DMP^+$ salt are about twice as large as for the mixed cation compound, and those for the CPA^+ salt are intermediate in value. This study demonstrates again that the $CuBr_4^{2-}$ anion/organic cation systems are rich in possibilities for a wide variety of structural and magnetic behavior. Just within the antiferromagnetic (AFM) ladder systems, by varying the cation one can produce compounds such as (5-iodo-2-aminopyridinium)$_2CuBr_4$[4c] and (piperidinium)$_2CuBr_4$,[4a,b] in which the rung exchange is much more than the rail exchange (13/1 for the 5-iodo-2-aminopyridinium salt), to the nearly equivalent values for the (5-nitro-2-aminopyridinium)$_2CuBr_4$ salt,[4d] and to strong rail systems mentioned above.

The analyses of exchange pathways are very complex in these $CuBr_4^{2-}$ salts, since multiple structural parameters are required to specify the interaction pathways. Most successful magneto-structural correlations are found in systems where structural constraints restrict the structural variations to only one or two parameters. This is not the situation in these salts. Most analyses of the exchange pathways have focused on the following parameters:[9a] (a) The Br···Br contact distance, (b) the *trans* Br−Cu−Br angles, (c) the Cu−Br···Br angles, and (d) the Cu−Br···Br−Cu torsion angle. However, a comparison of the structural parameters for the rung interactions in the DMA^+/$35DMP^+$ and the $23DMP^+$ salts show that these four parameters are not sufficient to define the nature of the pathway. In both cases, the $CuBr_4^{2-}$ anions involved in the rung interactions are related by centers of inversion, and the only structural parameter that is significantly different is the Br···Br contact distance.[26] This distance is 0.361 Å longer in the $23DMP^+$ salt, so the interaction is expected to be considerably weaker. However, the exchange coupling is twice as strong as in the DMA^+/$35DMP^+$ salt. Clearly, one or more additional parameters must be involved in defining these pathways.

A comparison of the structural features of the rung interactions in the two salts gives a clue as to an additional parameter that needs to be defined. The direction of the S_4 compression axes of the pseudo-D_{2d} groups of the $CuBr_4^{2-}$ anions is first determined by calculating the least-squares plane of the four bromine atoms. This is an important direction for defining the exchange interaction since the magnetic orbital will belong to an irreducible representation of the D_{2d} group. Figure 6 presents two different views of the rung interactions for the two salts. The top diagrams give edge-on views of the least-squares planes and perpendicular to the rung Br···Br contact distance, thus perpendicular to both the S_4 axis and the rung Br···Br contact distance with the S_4 axes vertical. The bottom diagrams give views parallel

(26) The trans Br−Cu−Br angles are somewhat smaller in the $(23DMP)_2CuBr_4$ salt (128° vs 137°) but this is not expected to make a significant difference in the magnetic orbitals.

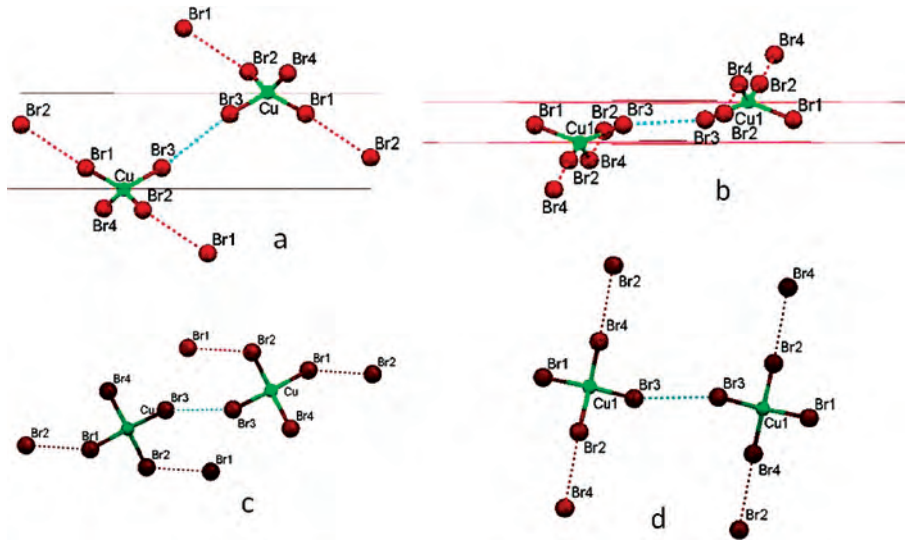

Figure 6. Diagrams illustrating the relative orientations of the S_4 axes and rung Br···Br contact distances for $(23DMP)_2CuBr_4$ (left-hand side) and (DMA)(35DMP)$CuBr_4$ (right-hand side). Top diagrams (a, b) are views perpendicular to both the S_4 axes (vertical) and the rung Br···Br contacts, with the S_4 axes vertical. Horizontal lines are planes perpendicular to the S_4 axes of the $CuBr_4^{2-}$ anions. Bottom diagrams (c, d) are views parallel to the S_4 axes obtained by rotating the top diagrams about a horizontal axis.

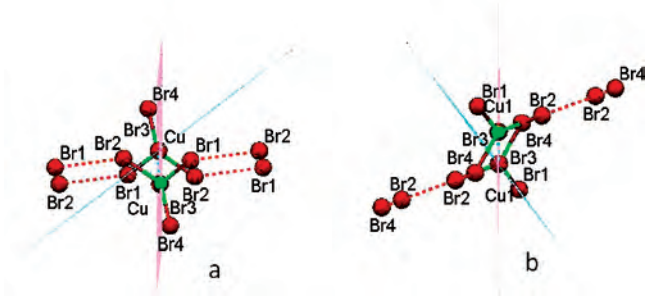

Figure 7. Diagram showing the orientation of the *trans* Br−Cu−Br···Br torsion angles for $(23DMP)_2CuBr_4$ (a, left) and (DMA)(35DMP)$CuBr_4$ (b, right) as viewed parallel to the intersection of the Br−Cu−Br plane (blue) and the Cu−Br···Br plane (pink).

to the S_4 axes, obtained by rotating the top views by 90° about a horizontal axis. In both sets of diagrams, the rail Br···Br contacts are shown to help define the ladder orientations. From the top diagrams, it is clear that the planes perpendicular to the S_4 axes are considerably closer together in the $DMA^+/35DMP^+$ salt (1.993 Å) than in the $23DMP^+$ salt (4.745 Å). As a consequence, the angle between the S_4 axes and the rung Br···Br contact distances are distinctly different, implying that the two pathways are significantly different despite the similarities in the traditional angular parameters.

A second difference between the rung interaction pathways in the two compounds is observed by calculating the *trans* Br−Cu−Br···Br torsion angle. As tabulated in Table 1, these values differ by ~90° between the two salts. This difference is illustrated in Figure 7. Here the two structures are compared by projecting the rung interactions down the intersection of the *trans* Br−Cu−Br plane (blue) and the Cu−Br···Br plane (pink). The latter is oriented vertically in the diagrams for both compounds. It is seen that, as a result of this difference in torsion angle, two *cis* Br−Cu−Br angles face each other in the $23DMP^+$ salt while two *trans* Br−Cu−Br angles are cofacial in the $DMA^+/35DMP^+$ salt.

This analysis shows that the factors that affect the two-halide exchange pathways in these $CuBr_4^{2-}$ systems are clearly very complex. The above analysis involved anions related by a center of inversion. For systems lacking this type of symmetry restrictions, the variables will be even more complex. This highlights the necessity of have good first principle bottom up calculation capabilities to clearly define the magnetic properties of these systems.

Acknowledgment. The Bruker (Siemens) SMART APEX diffraction facility was established at the University of Idaho with the assistance of the NSF-EPSCoR program and the M. J. Murdock Charitable Trust, Vancouver, WA, U.S.A. The MPMS-XL SQUID magnetometer was purchased with financial assistance from the NSF (IMR-0314773) and from the Kreske Foundation. R.D.W. appreciates the continuing support of the Department of Chemistry and the College of Science, Washington State University.

Supporting Information Available: Crystal data in CIF format. This material is available free of charge via the Internet at http://pubs.acs.org.

IC800905E